

FATIGUE FRACTURE OF THERMOMECHANICALLY PROCESSED  
LOW CARBON STEEL

R. L. Duffin\* and J. G. Byrne\*\*

## INTRODUCTION

Grange [1] has shown how the principles of fiber composite strengthening can be applied to low carbon steels. The idea of using fiber reinforcement to increase the tensile strength of a low carbon steel is quite different from the methods normally used. The object is not to interfere with dislocation movements by the addition of alloying elements or by precipitation hardening, but rather to use the plastic flow of the matrix under stress to transfer the load to the fibers by the means of shear stress. Using thermo-mechanical techniques, strong, fibrous microconstituents can be developed such that there is an improvement in the combination of strength, ductility and toughness. One such technique, described below, develops high carbon martensite fibers in a ferrite matrix.

Normalized 1020 steel contains about 22% pearlite in a ferrite matrix. This steel was cold rolled 75%, elongating the pearlite colonies into sheets parallel to the rolling plane. The steel was then heated to 1052 K, just slightly above the  $A_{c1}$  temperature of 1025 K, and held there for one minute. This brief hold above  $A_{c1}$  converted the pearlite sheets to austenite and recrystallized the ferrite matrix. The austenite inherited the high carbon content of the pearlite and transformed on quenching to sheets of high carbon martensite. The martensite-ferrite interface is irregular on a fine scale because of the shapes of the surrounding ferrite grains. This uneven interface should increase the adhesion between composite fiber and matrix thus adding to the effective composite efficiency. The composite behaviour reported by Grange [1] was most interestingly manifested by a concurrent increase of strength *and* ductility, properties which normally change in opposite directions. The current work was aimed at examining whether or not this advantageous static composite behaviour would carry over into the realm of dynamic fatigue behaviour.

## EXPERIMENTAL

Cantilever bending, constant maximum stress fatigue specimens were machined from steel sheet after rolling and the thermomechanical treatment (TMT) described above. S-N curves were produced using a Sonntag SF-2-U machine. Specimens processed to the fully hardened condition and the normalized condition were also examined. AISI 1020 steel sheet was fully hardened by austenitizing thirty minutes at 1230 K and brine quenching. Optical surface observations were made as a function of fatigue life to study crack development and propagation. The surfaces were initially polished and etched with 2% nital. Fracture surfaces were examined with a scanning electron microscope. Tensile properties were measured on an Instron testing

\* Kaiser Steel Corporation, Fontana, California, U. S. A.

\*\* University of Utah, Salt Lake City, Utah, U. S. A.

machine at a crosshead speed of 0.13 cm per minute. X-ray textural studies were performed on a Siemens pole figure goniometer in the reflection mode using Va filtered Cr radiation.

## RESULTS AND DISCUSSION

The texture of the 1020 steel after TMT can best be described as  $\{112\}\langle 111 \rangle$ , that is 112 planes of the ferrite are mostly parallel to the sheet surface and 111 directions are mostly in the rolling direction.

The effectiveness of the strengthening of the fibrous martensite could not be rigorously determined due to the irregular fiber shapes. In this case the best check was that strengthening did occur. Also, SEM examination of tensile specimen fracture surfaces gave no indication of the martensite being pulled out from the ferrite matrix. Two mechanisms of fracture were noted; namely, microvoid coalescence in the ductile ferrite and cleavage in the brittle martensite.

It was verified that the current work duplicated Grange's TMT process by tensile tests conducted on 1020 steel in both the as quenched TMT process and after a 477 K temper. These results are shown in Table 1 along with tensile test results for conventionally heat-treated 1020 steel. The tempered TMT steel possessed greater strength and only slightly lower ductility compared to the 1020 steel quenched and tempered at 811 K. The as quenched TMT steel showed slightly lower strength but significantly greater ductility compared to the fully hardened 1020 steel.

The S-N curves for normalized 1020 steel, TMT 1020 steel, and fully hardened 1020 steel are shown in Figure 1. The TMT steel showed a much better fatigue life than the normalized steel but was significantly poorer than the fully hardened steel. This could have been predicted based upon the ultimate tensile strengths of the materials. The ratio of the estimated fatigue limit to the tensile strength for the TMT steel and the fully hardened steel are almost identical. However, the S-N curve for TMT steel tempered at 477 K is almost identical to that of the untempered TMT steel which is stronger. The relation between UTS and the fatigue limit does not appear to hold in this case.

Figures 2a and 2b show crack development and propagation in a TMT 1020 cantilever specimen while being cycled at a maximum bending stress of 522 MPa. Initially slip bands formed in the ferrite matrix at an angle  $45^\circ$  to the stress axis. These bands eventually became short cracks which were succeeded by major crack growth perpendicular to the stress axis and independent of the microstructure. The stronger, untempered TMT steel did not show any better fatigue properties than did the weaker, tempered TMT steel. The same fatigue mechanism was observed in both materials. This same kind of slip band development and crack propagation was observed by Beardmore and Feltner [2] in low carbon, low alloy, martensitic steel. The transformation induced martensite contained a high density of dislocations arranged in a substructure with cell walls aligned with definite crystallographic arrangements. In their summary, they state that "the presence of a substructure which enhances the strength in unidirectional deformation may not be of similar benefit under cyclic straining conditions". A similar effect may cause the observed insensitivity of the fatigue limit to the tensile strength in the TMT steel.

A possible explanation for the lower fatigue life of the TMT 1020 compared to the fully hardened 1020 is that the former is composed of 74% ferrite of low strength and 26% martensite of high strength, whereas, the fully hardened steel is a more homogeneous microstructure in terms of strength than in the TMT case. During fatigue of the TMT steel stress concentrations could occur in the ferrite regions because of the strength and ductility differences between the ferrite and the 0.7% carbon content martensite. Slip in the ferrite would be a mechanism to relieve the bending stress.

A specimen of TMT 1020 steel was fatigued for  $3.7 \times 10^6$  cycles at 255 MPa, approximately 69 MPa below the fatigue endurance limit. No slip band formation or cracking was observed in the ferrite, suggesting that the fatigue limit is the minimum stress required to fracture the ferrite.

Fully hardened 1020 steel was stressed at 621 MPa in cyclic fatigue. No slip band or crack development was observed in the first 50,000 cycles. At 51,000 cycles, rapid crack propagation occurred as shown in Figure 3.

SEM details of the fatigue fracture surface of TMT 1020 steel are shown in Figure 4. Well defined cleavage is seen in the martensite fibers and microvoid coalescence is evident in the ferrite. The fully hardened fracture appearance, seen in Figures 5 and 6, is quite different from the TMT 1020 appearance in that considerable ductile fracture is evident and the brittle platelets of martensite exhibit smaller cleavage facets separated by tear ridges (quasi-cleavage).

Variations of the TMT process were made in an attempt to improve the fatigue life. The intercritical anneal time was increased from 2 to 20 minutes prior to quenching resulting in slightly reduced tensile strength with no appreciable change in fatigue life. However, a change in the temperature of the one minute intercritical anneal from 1025 K to 1044 K did produce a significant improvement in fatigue life at all stress levels examined. Tensile strengths were almost identical. Quenching from the higher temperature produced a mixture of 65% ferrite and 35% martensite of a lower carbon content (0.53%) than previously obtained. This martensite had a Vickers hardness of 810 compared with the previous (0.7%) martensite which had a Vickers hardness of 910. A smaller difference in strength (hardness) between the martensite and ferrite appeared to result in better fatigue behaviour.

Finally, non-oriented martensite in ferrite was produced by: 75% cold rolling, plus 30 minutes at 1025 K, plus a brine quench. This treatment resulted in about 26% non-oriented martensite of 0.7% carbon and 74% ferrite. A specimen fatigued at 531 MPa maximum stress failed exactly on the S-N curve of Figure 2; i.e., at 34,000 cycles. Slip bands had first been observed in the ferrite at 1000 cycles. This suggests that the orientation of the microstructure is less important than is the strength difference between the microconstituents.

## CONCLUSIONS

(1) As stated by Grange [1] the TMT processed low carbon steels have a better combination of strength and ductility than conventionally processed low carbon steels.

(2) The fatigue life of TMT 1020 steel, as quenched, is almost identical to that of the TMT 1020 steel after a 477 K temper, despite the large

difference in ultimate tensile strengths.

(3) An increase in the intercritical annealing temperature for TMT 1020 steel increases the fatigue life. It is felt that this is due to the decrease in carbon content of the martensite regions and the resulting lower strength difference between the martensite and the ferrite matrix.

(4) TMT low carbon steels fail in fatigue by the formation of slip bands in the ferrite matrix at an angle of 45° to the stress axis followed by the initiation of microcracks in the slip bands, and the eventual propagation of a major crack normal to the stress axis and independent of the microstructure.

ACKNOWLEDGEMENTS

The authors wish to acknowledge the support of the National Science Foundation, specifically the Latin American Cooperative Research Program. The U. S. Steel Corporation provided the materials used.

REFERENCES

1. GRANGE, R. A., Second International Conference on Strength of Metals and Alloys, Asilomar, 1970, 861.
2. BEARDMORE, P. and FELTNER, Second International Fracture Conference, 1969, 607.
3. "Properties of Some Metals and Alloys", INCO, Third Edition, 1968, 38.

Table 1 Mechanical Properties of 1020 Steel

CONDITION OF 1020 STEEL	0.2% OFFSET YIELD STRENGTH (MPa)	TENSILE STRENGTH (MPa)	% ELONGATION
TMT 1020, As Quenched	799	1007	11
TMT 1020, 477 K Temper	469	717	21
1020 Fully Hardened	806	1098	4
1020, Quenched and Tempered at 811 K [3]	428	621	25
1020, Annealed [3]	262	448	30

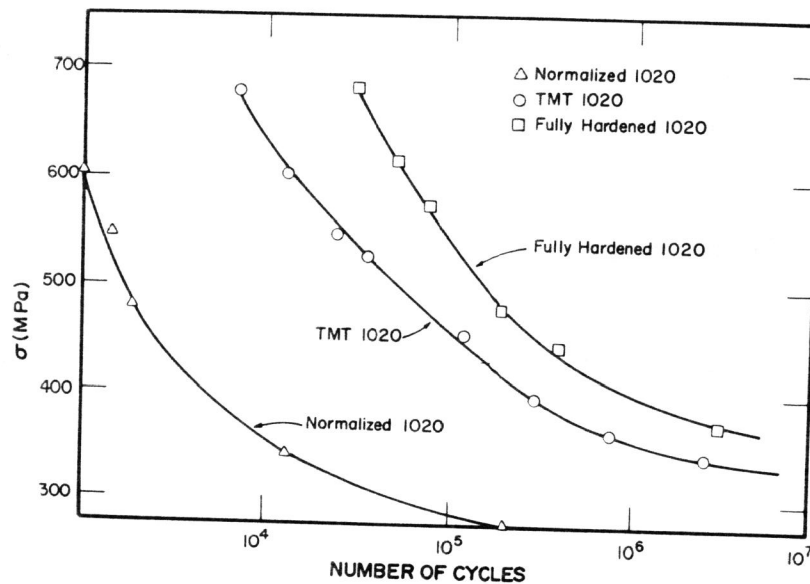
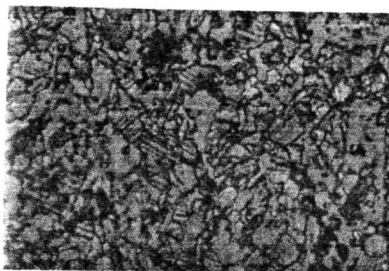
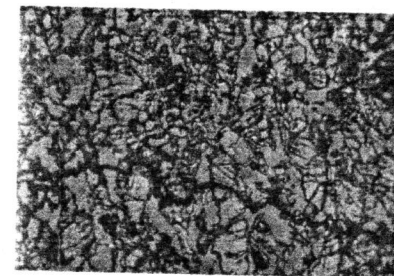


Figure 1 Plot of Cyclic Stress versus Number of Fatigue Cycles for Various Steel Treatments



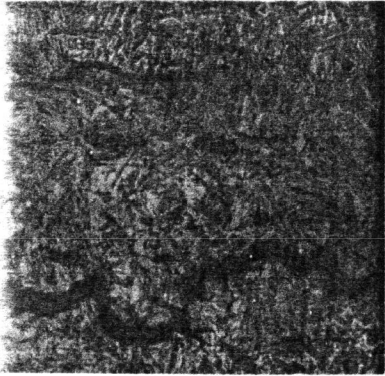
400X



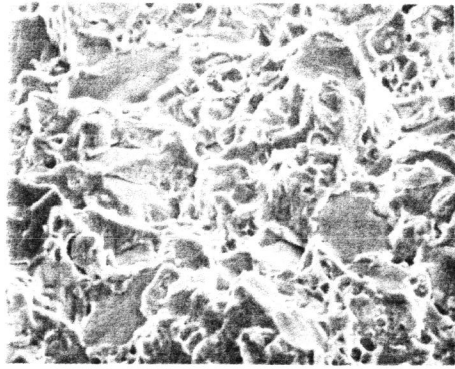
400X

Figure 2a TMT 1020 Steel after Fatiguing for 10,000 Cycles. Slip Bands well Developed in Ferrite

Figure 2b TMT 1020 Steel after Fatiguing for 24,000 Cycles. The Crack has Propagated in a Direction Normal to the Stress Axis and Independent of the Microstructure



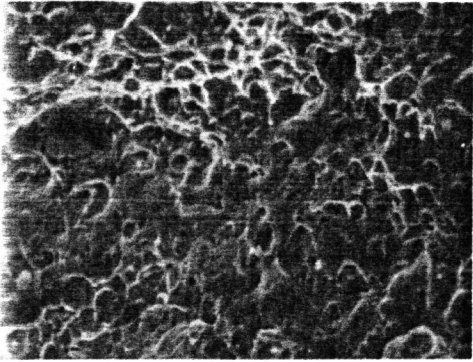
400X



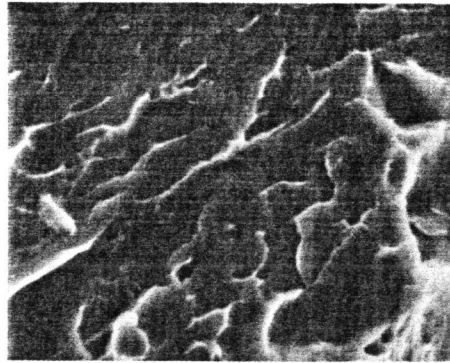
1000X

Figure 3 Fully Hardened 1020 Steel after Fatiguing for 51,000 Cycles. Cracks have Propagated Catastrophically

Figure 4 Fracture Surface of TMT 1020 Steel Cantilever Specimen as Observed in SEM



1125X



5500X

Figure 5 Representative SEM View of the Cantilever Fracture Surface of a Fully Hardened 1020 Steel

Figure 6 Higher SEM Magnification of Fracture in the Brittle Area in Fully Hardened 1020 Steel